

Broken Rotor Bar Fault Detection in Induction Motor Based on Spectral Analysis

Zafer Dogan

Abstract— Three-phase induction motors are among the most frequently used motors in industrial areas due to their simple structure, low cost, power specifications, etc. Electric energy consumption from these motors accounts for 68% of the energy used by all motors. The faults that occur in these motors over time decrease motor efficiency and result in significant energy consumption. In this study, a new method based on spectral subtraction (SS) was suggested for determining broken rotor bar (BRB) faults in these motors. The traditional method of motor current signature analysis via Fast Fourier Transform (FFT) is hard to use to diagnose BRB faults because the sideband characteristics used as a fault indicator are also seen in the healthy state at low amplitude levels. In the proposed fault detection method, the FFT of both healthy case and faulty case current signals were calculated and then the SS signal is obtained by subtracting the FFT of the healthy motor from the faulty motor for each time step. In the residual SS signal, fault detection was performed by examining the amplitude levels of the harmonic component of the BRB fault. Experimental results indicate that BRB faults can be successfully detected in squirrel-cage rotor induction motors using the suggested method.

Index Terms— Broken rotor bar, Induction motor, Spectral subtraction, Energy-saving, Induction motor energy consumption.

I. INTRODUCTION

ELECTRONIC ENERGY is among humanity's primary and indispensable needs. The most intense consumption of this energy is consumed due to electric motors. According to International Energy Agency (IEA) estimates, 53% (10,500 TWh per year) of the electricity consumed worldwide is consumed by electric motors. This consumption gives rise to around 6800 Kt of CO₂ emissions. Induction motors are the most preferred motor among electrical motors. These motors are driving machines that have been used for many years due to their simple structure, low cost and stable operation. These motors consume 68% of the energy used by all motors worldwide [1]. Any amount of energy saving in these motors is important for both the environment and the efficient use of primary resources due to their excessive consumption [2]. Despite induction motors strong and stable structure, various faults can occur because of thermal stress, magnetic

stress, production faults, dynamic stress, environmental conditions, etc. As shown in Fig. 1, induction motor faults can be classified, in general, as [3]: Stator faults (Open or Short Circuit in one or more phase windings), Rotor Faults (Broken Rotor Bar (BRB) and End-ring cracking), Bearing Faults (Outer race, Inner race, Ball and Cage failures), Other faults (Eccentricity faults, Shaft inclination and Driver based faults).

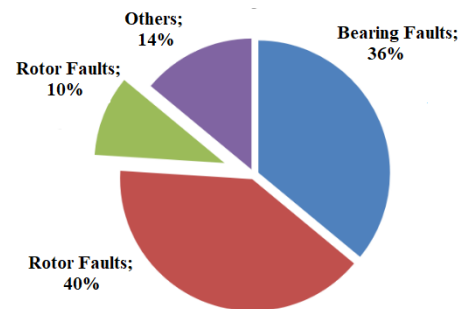



Fig.1. Induction motor faults[3]

Most 3-phase induction motors used in industrial areas have a squirrel cage rotor. Broken bar faults or end ring faults take place in this rotor over time. The rotor faults make up about 8–10% of all faults in induction motors. The main causes of rotor faults can be classified as losses and pores on the bars due to thermal overloading; noise-vibration due to irregular magnetic attractions; manufacturer faults; torque generated by the load on the motor shaft; frequent stops and starts; faults due to centrifugal and circular rotation; and faults due to environmental conditions such as moisture, chemicals and dirt [3], [4].

The faults in induction motors cause many adverse conditions, which are vibration and noise in the motor, heat increase in the motor, uneven air gap flux distribution, decrease and oscillation in average moment, decrease in efficiency, harmonics in the line current and induced electromotive force (EMF), etc[4], [5]. In terms of working safety, economy and energy savings, early detection of faults in the mechanical and electrical parts of induction motors is very important. Periodic maintenance operations performed at certain time intervals allow operating electrical motors for long periods of time without any fault. Currently, real-time condition monitoring and fault detection based predictive maintenance are replacing periodic maintenance. Therefore, monitoring electric motors and predictive maintenance are among the most important issues that are focused on today [5], [6], [7].

ZAFER DOGAN, is with Department of Electrical and Electronic Engineering University of Tokat Gaziosmanpaşa University, Tokat, Turkey. (e-mail: zafer.dogan@gop.edu.tr).

 <https://orcid.org/0000-0002-7953-0578>

Manuscript received Aug 15, 2024; accepted Oct 27, 2024.
DOI: [10.17694/bajece.1533675](https://doi.org/10.17694/bajece.1533675)

Many methods, such as motor current signals [8], [9], vibration [10], instantaneous power [3], noise, chemical analysis etc., are used for fault detection in these motors. Motor current signature analysis (MCSA) is the most frequently used method among these methods [11]. The motor current signal can be monitored non-invasively. The traditional MCSA method is quite successful, especially for motors operating under constant speed, constant load torque and constant voltage [12]. There are many studies in the literature for detecting BRB faults in induction motors via MCSA [8], [9], [13], [14], [15], [16], [17], [18]. When BRB occurs in the motor, the frequency spectrum of the motor stator phase currents changes from the healthy state [19]. Many methods based on analysis of the stator currents have been used in detecting induction motor BRB faults. Among them, time-domain analysis [20], frequency domain analysis [3], [4], [5], [11], [14], [21] and time-frequency domain analysis [7], [9], [18], [22], [23] are the most well-used methods. Although time-domain analyses are practical, they may not always produce the desired diagnostic results. In contrast to time domain analysis, time-frequency domain analysis is impractical but can produce the desired diagnostic results. Frequency domain analysis is both partially practical and can give the desired diagnostic results [3], [4]. In frequency domain analysis, time domain signals are transmitted to the frequency spectrum via Fourier transforms. In a Fourier transform method, the spectrum of the monitored current signal is analyzed, and the frequency components of the signal are examined. Researchers using this method have monitored the sideband components to the lower and upper components of the fundamental frequency for BRB fault detection. In [5], a Fast Fourier transform (FFT)-based BRB fault diagnosis was made using an MCSA in an induction motor driven by an inverter. The fault detection was implemented using characteristic frequencies of the BRB fault in a fuzzy logic algorithm. In [24], a support vector machine (SVM) was used to detect BRB in induction motors. The curve area, crest angle and amplitude of harmonics were extracted from the stator current using FFT. Then, these fault characteristics were applied to the SVM input and a fault diagnosis was made. It is difficult to diagnose BRB faults using the FFT of the motor current signals because the sideband characteristics used as a fault indicator are also seen in the healthy state at low amplitude levels. Therefore, classification algorithms are used in most of the BRB studies. This problem can also be resolved using a spectral subtraction (SS) method. The SS method is widely used for removing acoustic noise in audio data processing [22], [25], [26]. Spectral subtraction is a good tool for reducing the spectral effect of healthy motor spectral components on the stator phase current [22].

In this study, a new approach is presented for BRB fault detection in induction motors using stator current SS. The main purpose of this study was to detect these faults at the initial stage. The stator phase current of the motor is monitored to

obtain the SS signal. The SS signal is obtained by subtracting the spectral components of the healthy motor from the faulty motor for each time step. Fault diagnosis was performed by statistical analysis of the SS signal.

The study is comprised of 5 sections. The 2nd section after the Introduction explains the impacts of BRB faults on induction motors. Section 3 focuses on the calculation of motor current SS signal values for both the healthy and faulty cases. Experimental studies are presented in Section 4. Results are presented in Section 5.

II. BROKEN ROTOR BAR DETECTION BY MCSA

In a healthy condition, an induction motor operates under uniformly distributed mechanical and electromagnetic forces. The impedances of the stator equivalent windings of the motor are identical. For the healthy case, a squirrel-cage rotor resistance matrix $[R_r]$ is given as [27]

$$[R_r] = \begin{bmatrix} 2(r_b + r_e) & -r_b & 0 & \dots & 0 & 0 & -r_b & r_e \\ -r_b & 2(r_b + r_e) & -r_b & \dots & 0 & 0 & 0 & r_e \\ \vdots & \vdots & \vdots & \vdots & \vdots & \vdots & \vdots & \vdots \\ \vdots & \vdots & \vdots & \vdots & \vdots & \vdots & \vdots & \vdots \\ 0 & 0 & 0 & \dots & -r_b & 2(r_b + r_e) & -r_b & r_e \\ -r_b & 0 & 0 & \dots & 0 & -r_b & 2(r_b + r_e) & r_e \\ -r_e & -r_e & -r_e & \dots & -r_e & -r_e & -r_e & -nr_e \end{bmatrix} \quad (1)$$

where r_e is the resistance of the end-ring segment, r_b is the nominal resistance of the rotor bar and n is the number of rotor bars in the cage. As a result, under normal conditions, the stator phase currents of an induction motor with 3-phase squirrel-cage are symmetrical and the motor works with s slip at f source frequency. These currents produce a rotating magnetic field in the stator of the induction motor, as seen in Eq. (2) [27]

$$i_f = I_f \cos(\omega t - a_f) \quad (2)$$

where I_f represents amplitude, a_f fault condition component and i_f denotes the stator phase current. These rotating magnetic fields induce an EMF at frequency, s_f in the rotor circuit. A symmetric magnetic flux distribution is generated in the air gap when the stator and rotor circuits are symmetrical.

Rotor faults may develop in these motors when operating under extreme operating conditions due to thermal, magnetic, dynamic and environmental causes as well as mechanical and production faults. BRB and end-rings in induction motors are among the most important squirrel-cage rotor faults [22]. A BRB fault in an induction motor with a squirrel cage rotor changes the rotor equivalent circuit of the motor. To model the impact of the broken bar, a defect resistance, r_{bb} , is added to the rotor resistance matrix, $[R_r]$. As a result, the squirrel-cage rotor equivalent resistance matrix, $[R_{rb}]$, accounting for the impact of the broken bar, is defined by Eq. (3) [9].

$$[R_{rb}] = \begin{bmatrix} 2(r_b + r_e) & -r_b & 0 & \dots & \dots & 0 & 0 & -r_b & -r_e \\ -r_b & 2(r_b + r_e) & -r_b & \dots & \dots & 0 & 0 & 0 & -r_e \\ 0 & \ddots & \ddots & \ddots & \dots & \dots & \dots & \dots & -r_e \\ \vdots & 0 & -r_b & (2(r_b + r_e) + r_{bb}) & (-2(r_b + r_e) - r_{bb}) & 0 & \dots & \dots & -r_e \\ \vdots & \vdots & 0 & (-2(r_b + r_e) - r_{bb}) & (2(r_b + r_e) + r_{bb}) & -r_b & 0 & \dots & -r_e \\ \vdots & \vdots & \vdots & \ddots & \ddots & \ddots & \vdots & \dots & -r_e \\ 0 & 0 & 0 & \dots & \dots & -r_b & 2(r_b + r_e) & -r_b & -r_e \\ -r_b & 0 & 0 & \dots & \dots & 0 & -r_b & 2(r_b + r_e) & -r_e \\ -r_e & -r_e & -r_e & -r_e & -r_e & -r_e & -r_e & -r_e & -nr_e \end{bmatrix} \quad (3)$$

The phase currents flow from the stator windings under BRB conditions [27];

$$i_{(1-s)f} = I_{(1-s)f} \cos((1 - 2s)\omega t - a_{(1-s)f}) \quad (4)$$

where $I_{(1-2s)f}$ represent amplitude and $i_{(1-2s)f}$ represents the stator phase current increasing due to rotor asymmetry. These currents result in the generation of two magnetic fluxes rotating contrary to one another at frequencies $\pm sf$ subject to the rotor circuit asymmetry as well as the generation of an oscillating stator EMF at frequency component $(1 - sf)$ [27]. As a result, it begins a speed oscillation and a vibrating torque at the frequency $2sf$ [28]. The propagation of the BRB fault in the frequency domain is shown in Fig. 2.

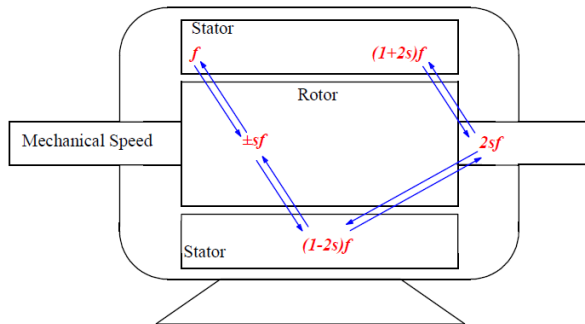


Fig. 2. The propagation of the BRB fault in the frequency domain

The electrical and magnetic asymmetries in the rotor also generate harmonics at the sidebands of the source frequency in the motor phase current. BRB harmonic components can be calculated via spectral analysis of the motor currents. The BRB frequency components can be given as [3], [4]:

$$f_b = (1 \pm 2s)f \quad (5)$$

where f_b represents the broken rotor bar frequency and s is the slip.

The frequency components of the sidebands that represent BRB faults change dynamically with the load moment of the motor. Hence, this change should be taken into consideration when applying SS and the differences of the motor phase current signals under the same load conditions should be calculated when determining the healthy and faulty motor SS signal values. To do this, the sideband frequency harmonic components for BRB fault should be determined accurately. These harmonic components depend on the slip value generated according to the load condition of the motor. For any load

moment of an induction motor, the slip value can be calculated precisely depending on the rotor speed [29]. For this purpose, the synchronous speed of the motor, n_s , can be calculated using Eq. (6) depending on source frequency and the number of poles. Depending on the calculated n_s and the rotor speed, n_r , obtained experimentally, slip can be calculated using Eq. (7). The term color space refers to the entire sum of colors that can be represented within the said medium. For our purposes,

$$n_s = 120. f / p \quad (6)$$

$$s = n_s - n_r / n_s \quad (7)$$

III. SPECTRAL SUBTRACTION ON THE MOTOR CURRENT SIGNALS

The SS method is frequently used to filter the noise generated in the sound signals for improving the sound quality but reference [30] shows that it has also been used successfully for bearing fault detection in electrical motors. The offered method gives highly successful results especially for induction motors that are running steady state.

Fig. 1 shows the topology of the method suggested for BRB fault detection of induction motors. This topology comprises five stages: data acquisition, normalization, FFT, Spectral subtraction, and feature extraction.

Signals are carried over to the frequency domain in spectral analyses. Fourier transformations are among the most frequently used spectral analysis methods [10]. Fourier transformation, which is used in many scientific areas for harmonics analysis, is also an important fault detection tool for the detection of faults in electrical motors. Since the signals used for fault detection in electrical motors include a limited number of samples within a certain time interval, Discrete Fourier Transformation (DFT) is used in these applications [4]. DFT can be expressed as in Eq (8)

$$X(k) = \sum_{n=0}^{N-1} x(n)e^{-j2\pi \frac{k}{N}n}, k = 0,1,\dots, N - 1, \quad (8)$$

where N denotes the length of the x signal which contains a certain number of samples.

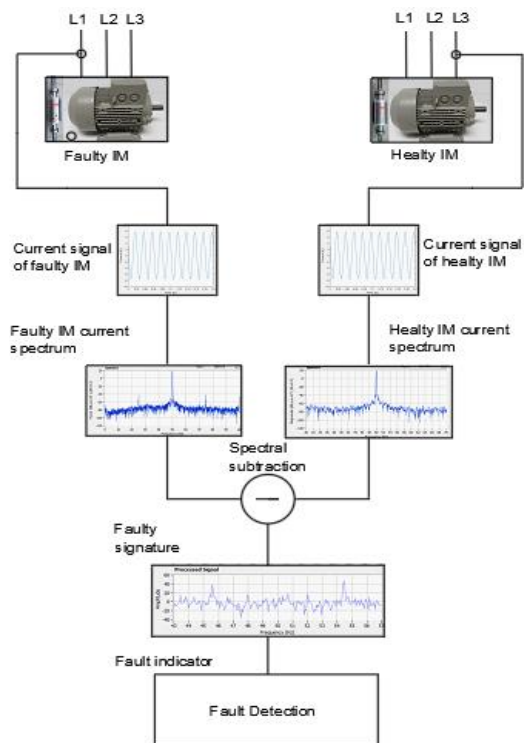


Fig.3. Block diagram for the suggested fault detection method

In this study, the application stages of the proposed SS method for diagnosing BRB faults are as follows:

1. The stator phase current signals acquired from healthy and faulty motors are normalized, after which $xh(n)$, the healthy motor current signal, and $xf(n)$, the faulty motor current signal, are obtained.
2. $xh(n)$ and $xf(n)$, each containing N samples, are windowed using a Hanning window. Thus, $xhw(n)$, the windowed healthy motor current signal, and $xfw(n)$, the windowed faulty motor current signal, are generated.
3. The current spectrums of $Xfh(k)$, healthy motor, and $Xff(k)$, faulty motor, are calculated by replacing $xhw(n)$ and $xfw(n)$ signals in Eq. (8).
4. The SS signal, $R(k)$, seen in Eq. (9), is obtained by subtracting the FFT of the healthy machine from the faulty machine for each time step [25]. The most important feature of the SS signal obtained here is that it carries only the fault effects of the motor current.

$$R(k) = \|Xfh(k) - Xff(k)\| \tag{9}$$

5. The BRB fault status in IM can be calculated using Eq. (10). The difference between the amplitude response, $A(f)$, corresponds to the frequency, f , and the amplitude response, $A((1 \pm 2s)f)$, corresponds to the frequency, $(1-2s)f$, in the $R(k)$ SS signal. The difference value, D , can be given as,

$$D = A((1 \pm 2s)f) - A(f). \tag{10}$$

Accordingly, the motor is faulty if $D > 0$.

IV. EXPERIMENTAL STUDY

The experimental setup used in the study is given in Fig. 4. The hardware used in this setup is comprised of an induction motor, DC machine, data acquisition system and tachometer. The DC Machine used as a load in this system has a loading capacity of 2800 rpm and 42 Nm. The torque sensor is in a strain gage structure and has a measurement capacity of 100 Nm.

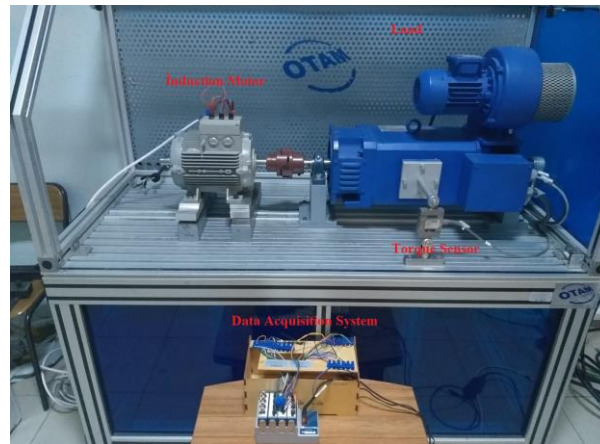


Fig. 4. Experimental setup

Two identical induction motors were used during the experiments for the healthy motor and faulty motor states. Table.1 shows the parameters of the motor used in the experimental studies.

TABLE I THE PARAMETER OF THE INDUCTION MOTOR	
Rated output power	2.2 kW
Supply frequency	50 Hz
Supply phase voltage	230/400 V (Δ/Y)
Rated current	8.4/4.85 A (Δ/Y)
Rated speed	1435/min
Power factor	0.82
Efficiency	79.7%

The load conditions for the motor were generated using a DC Generator. High sampling frequency motor current data should be collected for BRB fault detection based on the SS signal. This study used a data acquisition system comprised of a National Instrument cDAQ-9174 cabin and NI 9227 current module to meet this demand. An optical tachometer was used to measure the rotor speed.

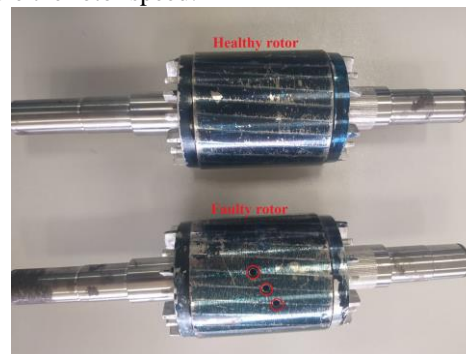


Fig. 5. Healthy and broken rotor bars

The BRB faults of the induction motors were generated artificially on the squirrel-cage rotor. The induction motor used in experimental studies had a total of 28 rotor bars. A 17 mm hole was drilled in one of the rotor bars using a 6 mm drill bit. Hence, one broken rotor bar (1BRB) was formed. The same operation was repeated for the other faults (2BRB, 3BRB). The rotors used in the experimental setup can be seen in Fig. 5. The motor phase currents were recorded for 20 s at a 25600 Hz sampling frequency. The data were monitored for 4 different states (healthy, 1 BRB, 2 BRB and 3 BRB) of the motor. Each motor state was tested in 6 different load conditions (0%, 25%, 50%, 75%, 100% and 115%). Fig. 6 shows the motor phase current signals for the healthy (IH), 1 BRB (I1BRB), 2 BRB (I2BRB) and 3 BRB (I3BRB) states.

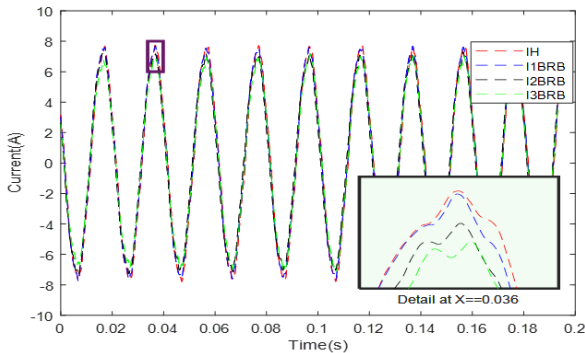


Fig.6. Stator phase current signals for induction motors faulty and healthy.

Fig. 6 shows that the sinusoidal form of the motor current signals deteriorates in case of BRB failure and this deterioration increases in direct proportion to the failure level. The main reason for this distortion is the harmonics caused by rotor failure.

V. RESULTS

The first stage in the fault detection process is distinguishing whether the motor is faulty. In this study, a data set of 512000 elements was created for fault detection from the phase current signals monitored in each motor load condition. Then, FFTs were calculated for the data sets using the Hanning window. Fig.7 shows, according to load conditions, the lower and upper sidebands, $((1 \pm 2s)f)$, of the fundamental frequency for BRB faults.

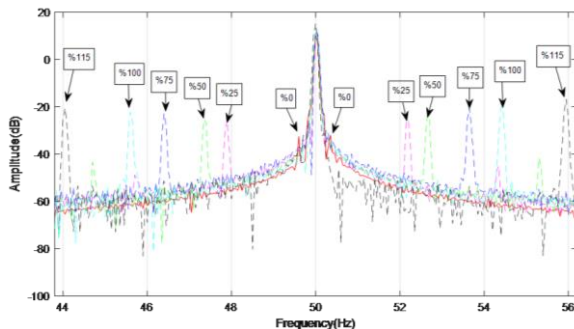


Fig.7. Frequency spectrums of different load currents for the 1BRB motor state. The harmonic frequency value corresponding to the RBB fault

in induction motors varies depending on the load condition of the motor. This change is clearly seen in Fig. 7. The respective 1BRB fault harmonic frequency components for 0%, 25%, 50%, 75%, 100% and 115% load conditions are 49.66–50.35 Hz, 47.8–52.2 Hz, 47.31–52.65 Hz, 46.39–53.65 Hz, 45.65–54.4 Hz and 44.14–55.95 Hz. The main reason for this change is the slip. The other words, the slip value of the motor changes with changing load conditions in induction motors.

The load conditions of the healthy motor and the faulty motor are the same in the SS-based induction motor fault detection method. In this study, the slip value corresponding to the load condition of the induction motor was calculated using Eq. (7), depending on the motor speed measured by a tachometer. Table II shows the slip and speed values depending on the load condition of the motor.

TABLE II
THE SLIP AND THE SPEED VALUES DEPENDING ON THE LOAD CONDITION OF THE MOTOR.

Load	Speed (rpm)	Slip
%0	1494.9	0.0034
%25	1467	0.022
%50	1459.65	0.0269
%75	1445.85	0.0361
%100	1435	0.0435
%115	1413,6	0,0576

At the last stage, the SS signals were calculated. As can be seen from Table 2, the change of the load case changes the slip value. Therefore, SS values are calculated according to each load case. Fig. 8 shows the 1BRB-Healthy SS signal, R1BRB(k), the 2BRB-Healthy signal, SS R2BRB(k) and the 3BRB-Healthy signal, SS R3BRB(k) figures for the motor under 100% load.

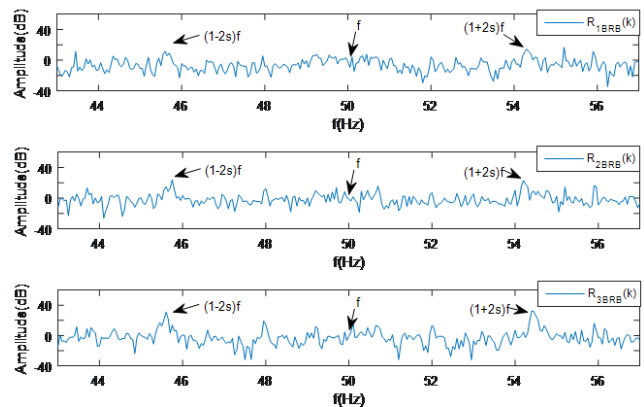


Fig.8. The SS signals under 100% load

In all the graphs in Fig. 8 the amplitude values at frequency f are approximately 0. This figure also shows that the amplitude values at frequencies f have larger BRB harmonic components than the amplitude values at frequencies f . Therefore, the motor has a BRB fault in all these graphs since $D > 0$.

Determining the fault level is the second important step in the fault detection process. Since hardware damage in the motor may increase with increasing fault level, increased fault level may result in an adverse situation, such as making the motor

completely unusable. Since an increase in the number of broken bars in the rotor will increase the total resistance, the amplitudes of the fault harmonic components of the motor stator currents in the frequency domain will also increase. Therefore, BRB fault levels can be easily determined by comparing the amplitude values for the harmonic frequencies of the SS signal. The amplitude values of the SS signal under different load conditions are shown in Fig.9.

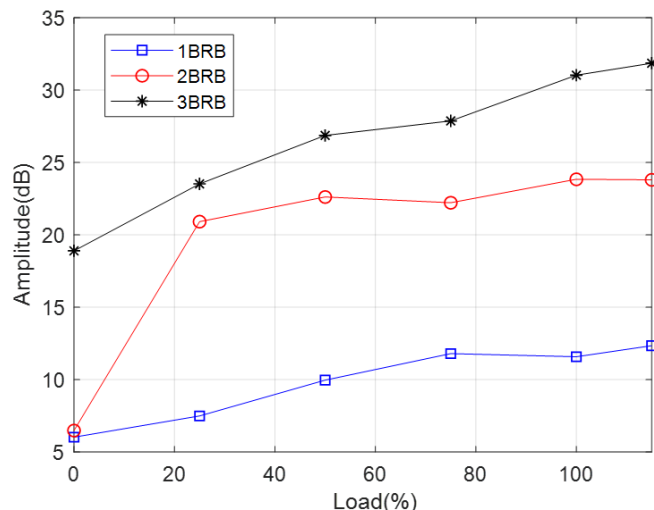


Fig.9. Amplitude values of the SS signal under different load conditions

This figure shows the amplitude values of the SS signals under 100% load condition as BRB1 11.579 dB, RB2 23.834 dB and BRB3 31.033dB. The different fault level values given for the 100% load condition are also similar for the other load conditions. These changes in harmonic amplitudes, which vary in direct proportion to the fault level, indicate the fault levels.

Many studies in the past years on the detection of conventional FFT-based BRB failures in induction motors have shown that rotor failure detection at 0% load condition is almost impossible [31]. In this study, under the 0% load condition, the amplitude values of the SS signals are 6.15 dB, 7.22 dB, and 18.02 dB for 1BRB, 2BRB and 3BRB fault conditions, respectively. According to these results, the proposed fault detection method can distinguish the fault level even under 0% load condition.

VI. CONCLUSION

This article focuses on BRB fault detection in a 2.2 kW three-phase induction motor. A new fault detection method based on the induction motor SS signal was suggested in this study. Induction motors stator phase currents were first monitored under 6 different load conditions in the healthy case. Afterwards, this monitoring procedure was repeated for the artificially generated 1BRB, 2BRB and 3BRB fault states. Spectral analyses were then carried out for the recorded motor phase current signals for each motor state. Finally, the SS signal values were calculated for the healthy state and for each fault status. BRB fault and fault level detection according to harmonic components at the sidebands of the motor's source frequency were carried out using the acquired SS signal values.

In addition, as a significant advantage of the suggested method, while 1BRB faults cannot be detected by most fault detection methods since a very low current passes through the rotor circuit in the 100 % load condition of an induction motor, fault detection could be carried out easily with this method. The results indicate that the suggested SS signal method can be successfully used for BRB fault detection in induction motors.

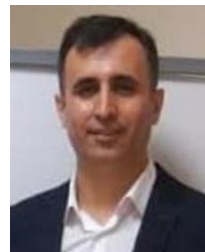
As a general result, the rapid and reliable fault detection achieved by the proposed method in induction motors, which are the most widely used in industrial areas all over the world and consume the most energy, will have an important contribution to humanity in terms of both economic and environmental aspects. The proposed method can be used in future studies to detect other faults in these motors.

REFERENCES

- [1] S. M. Lu, "A review of high-efficiency motors: Specification, policy, and technology," *Renewable and Sustainable Energy Reviews*, vol. 59, pp. 1–12, Jun. 2016, doi: 10.1016/j.rser.2015.12.360.
- [2] E. C. Bortoni, J. V. Bernardes, P. V. V. da Silva, V. A. D. Faria, and P. A. V. Vieira, "Evaluation of manufacturers strategies to obtain high-efficient induction motors," *Sustainable Energy Technologies and Assessments*, vol. 31, pp. 221–227, Feb. 2019, doi: 10.1016/J.SETA.2018.12.022.
- [3] "Electric Machines: Modeling, Condition Monitoring, and Fault Diagnosis - Hamid A. Toliyat, Subhasis Nandi, Seungdeog Choi, Homayoun Meshgin-Kelk - Google Books." Accessed: Feb. 28, 2024. [Online]. Available: https://books.google.com.tr/books?hl=en&lr=&id=JDSP3hCo9sUC&oi=fnd&pg=PP1&dq=info:D4vov8eNTewJ:scholar.google.com&ots=dk1uPvwfRZ&sig=AkxPS9U6Cqvsb08w--YHBZKixQM&redir_esc=y#v=onepage&q&f=false
- [4] S. Nandi, H. A. Toliyat, and X. Li, "Condition monitoring and fault diagnosis of electrical motors - A review," *IEEE Transactions on Energy Conversion*, vol. 20, no. 4, pp. 719–729, Dec. 2005, doi: 10.1109/TEC.2005.847955.
- [5] M. Akar and I. Cankaya, "Broken rotor bar fault detection in inverter-fed squirrel cage induction motors using stator current analysis and fuzzy logic," *Turkish Journal of Electrical Engineering and Computer Sciences*, vol. 20, no. 7, pp. 1077–1089, Jan. 2012, doi: 10.3906/elk-1102-1050.
- [6] M. Akar, "Detection of a static eccentricity fault in a closed loop driven induction motor by using the angular domain order tracking analysis method," *Mech Syst Signal Process*, vol. 34, no. 1–2, pp. 173–182, Jan. 2013, doi: 10.1016/J.YMSSP.2012.04.003.
- [7] Ç. BAKIR, "Different Induction Motor Faults by New Proposed Random Forest Method," *Balkan Journal of Electrical and Computer Engineering*, vol. 11, no. 4, pp. 380–386, Dec. 2023, doi: 10.17694/BAJECE.1283336.
- [8] F. Filippetti, M. Martelli, G. Franceschini, and C. Tassoni, "Development of expert system knowledge base to on-line diagnosis of rotor electrical faults of induction motors," *Conference Record - IAS Annual Meeting (IEEE Industry Applications Society)*, vol. 1992-January, pp. 92–99, 1992, doi: 10.1109/IAS.1992.244459.
- [9] M. Abd-el-Malek, A. K. Abdelsalam, and O. E. Hassan, "Induction motor broken rotor bar fault location detection through envelope analysis of start-up current using Hilbert transform," *Mech Syst Signal Process*, vol. 93, pp. 332–350, Sep. 2017, doi: 10.1016/J.YMSSP.2017.02.014.
- [10] Z. Wang, J. Yang, H. Li, D. Zhen, Y. Xu, and F. Gu, "Fault Identification of Broken Rotor Bars in Induction Motors Using an Improved Cyclic Modulation Spectral Analysis," *Energies 2019, Vol. 12, Page 3279*, vol. 12, no. 17, p. 3279, Aug. 2019, doi: 10.3390/EN12173279.
- [11] N. Mehala and R. Dahiya, "Motor Current Signature Analysis and its Applications in Induction Motor Fault Diagnosis,"

- [12] R. R. Schoen and T. G. Habetler, "A NEW METHOD OF CURRENT-BASED CONDITION MONITORING IN INDUCTION MACHINES OPERATING UNDER ARBITRARY LOAD CONDITIONS," *Electric Machines And Power Systems*, vol. 25, no. 2, pp. 141–152, Feb. 1997, doi: 10.1080/07313569708955729.
- [13] A. Bellini, F. Filippetti, G. Franceschini, C. Tassoni, and G. B. Kliman, "Quantitative evaluation of induction motor broken bars by means of electrical signature analysis," *IEEE Trans Ind Appl*, vol. 37, no. 5, pp. 1248–1255, Sep. 2001, doi: 10.1109/28.952499.
- [14] W. T. Thomson and M. Fenger, "Current signature analysis to detect induction motor faults," *IEEE Industry Applications Magazine*, vol. 7, no. 4, pp. 26–34, Jul. 2001, doi: 10.1109/2943.930988.
- [15] C. Delmotte-Delforge, H. Hénao, G. Ekwe, P. Brochet, and G. A. Capolino, "Comparison of two modeling methods for induction machine study: Application to diagnosis," *COMPEL - The International Journal for Computation and Mathematics in Electrical and Electronic Engineering*, vol. 22, no. 4, pp. 891–908, 2003, doi: 10.1108/03321640310482887/FULL/PDF.
- [16] P. Kołodziejek and E. Bogalecka, "Broken rotor bar impact on sensorless control of induction machine," *COMPEL - The International Journal for Computation and Mathematics in Electrical and Electronic Engineering*, vol. 28, no. 3, pp. 540–555, 2009, doi: 10.1108/03321640910940837/FULL/PDF.
- [17] S. Guedidi, S. E. Zouzou, W. Laala, K. Yahia, and M. Sahraoui, "Induction motors broken rotor bars detection using MCSA and neural network: Experimental research," *International Journal of System Assurance Engineering and Management*, vol. 4, no. 2, pp. 173–181, Mar. 2013, doi: 10.1007/S13198-013-0149-6/FIGURES/23.
- [18] H. Keskes and A. Braham, "Recursive Undecimated Wavelet Packet Transform and DAG SVM for Induction Motor Diagnosis," *IEEE Trans Industr Inform*, vol. 11, no. 5, pp. 1059–1066, Oct. 2015, doi: 10.1109/TII.2015.2462315.
- [19] O. Abdi Monfared, A. Doroudi, and A. Darvishi, "Diagnosis of rotor broken bars faults in squirrel cage induction motor using continuous wavelet transform," *COMPEL - The International Journal for Computation and Mathematics in Electrical and Electronic Engineering*, vol. 38, no. 1, pp. 167–182, Jan. 2019, doi: 10.1108/COMPEL-11-2017-0487/FULL/PDF.
- [20] B. Asad, T. Vaimann, A. Rassölk, A. Kallaste, and A. Belahcen, "Review of Electrical Machine Diagnostic Methods Applicability in the Perspective of Industry 4.0," *Electrical, Control and Communication Engineering*, vol. 14, no. 2, pp. 108–116, Dec. 2018, doi: 10.2478/ECCE-2018-0013.
- [21] B. Asad, T. Vaimann, A. Kallaste, and A. Belahcen, "Harmonic spectrum analysis of induction motor with broken rotor bar fault," *2018 IEEE 59th Annual International Scientific Conference on Power and Electrical Engineering of Riga Technical University, RTUCON 2018 - Proceedings*, 2018, doi: 10.1109/RTUCON.2018.8659842.
- [22] K. C. Deekshit Kompella, M. Venu Gopala Rao, and R. Srinivasa Rao, "Bearing fault detection in a 3 phase induction motor using stator current frequency spectral subtraction with various wavelet decomposition techniques," *Ain Shams Engineering Journal*, vol. 9, no. 4, pp. 2427–2439, Dec. 2018, doi: 10.1016/J.ASEJ.2017.06.002.
- [23] O. Abdi Monfared, A. Doroudi, and A. Darvishi, "Diagnosis of rotor broken bars faults in squirrel cage induction motor using continuous wavelet transform," *COMPEL - The International Journal for Computation and Mathematics in Electrical and Electronic Engineering*, vol. 38, no. 1, pp. 167–182, Jan. 2019, doi: 10.1108/COMPEL-11-2017-0487/FULL/PDF.
- [24] M. G. Armaki and R. Roshanfekar, "A new approach for fault detection of broken rotor bars in induction motor based on support vector machine," *Proceedings - 2010 18th Iranian Conference on Electrical Engineering, ICEE 2010*, pp. 732–738, 2010, doi: 10.1109/IRANIANCEE.2010.5506976.
- [25] S. V. Vaseghi, "Advanced Signal Processing and Digital Noise Reduction," *Advanced Signal Processing and Digital Noise Reduction*, 1996, doi: 10.1007/978-3-322-92773-6.
- [26] S. F. Boll, "Suppression of Acoustic Noise in Speech Using Spectral Subtraction," *IEEE Trans Acoust*, vol. 27, no. 2, pp. 113–120, 1979, doi: 10.1109/TASSP.1979.1163209.
- [27] P. Shi, Z. Chen, Y. Vagapov, and Z. Zouaoui, "A new diagnosis of broken rotor bar fault extent in three phase squirrel cage induction motor," *Mech Syst Signal Process*, vol. 42, no. 1–2, pp. 388–403, Jan. 2014, doi: 10.1016/J.YMSSP.2013.09.002.
- [28] A. Stefani, A. Yazidi, C. Rossi, F. Filippetti, D. Casadei, and G. A. Capolino, "Doubly fed induction machines diagnosis based on signature analysis of rotor modulating signals," *IEEE Trans Ind Appl*, vol. 44, no. 6, pp. 1711–1721, 2008, doi: 10.1109/TIA.2008.2006322.
- [29] S. Günel, D. G. Ece, and Ö. N. Gerek, "Zaman bölgesinde akim analizyle indüksiyon motoru hata tespiti," *2009 IEEE 17th Signal Processing and Communications Applications Conference, SIU 2009*, pp. 488–491, 2009, doi: 10.1109/SIU.2009.5136439.
- [30] E. H. El Bouchikhi, V. Choqueuse, and M. E. H. Benbouzid, "Current frequency spectral subtraction and its contribution to induction machines' bearings condition monitoring," *IEEE Transactions on Energy Conversion*, vol. 28, no. 1, pp. 135–144, 2013, doi: 10.1109/TEC.2012.2227746.
- [31] A. Kabul and A. Ünsal, "Diagnosis of simultaneous broken rotor bars and static eccentricity faults of induction motors by analyzing stator current and vibration signals," *Journal of the Faculty of Engineering and Architecture of Gazi University*, vol. 36, no. 4, pp. 2011–2023, 2021, doi: 10.17341/gazimfd.697785.

BIOGRAPHIES



Zafer DOĞAN was born in Tokat, Turkey, in 1974. He received the B.S. and M.S. degree in electrical education from Marmara University, Technical Education Faculty, Istanbul, Turkey, in 1996 and 2009, respectively. He is currently an Associate Professor in the Department of Electrical and Electronics Engineering, Tokat Gaziosmanpaşa University Faculty of Engineering and Architecture. His research interests are the design of electrical machines and fault diagnosis in electrical machines.